L'émission haute énergie des pulsars:

une conséquence de la reconnexion magnétique dans le vent strié?

Jérôme Pétri

Observatoire Astronomique de Strasbourg
Université de Strasbourg

Outline

UNIVERSITÉ DE STRASBOURG

Qu’est-ce qu’un pulsar?

1. étoile à neutrons
   objet compact de compacité $\frac{R_s}{R_*} \approx 0.4$
   $\Rightarrow$ effets de champ gravitationnel fort
2. fortement magnétisée
   $\Rightarrow$ plasmas quantiques, effets d’EDQ
   (création de paires $e^{\pm}$, raies cyclotron)
3. en rotation plus ou moins rapide
   $\Rightarrow$ intense champ électrique induit
   $\Rightarrow$ accélération violente de particules

Magnétosphère des pulsars: généralités

Qu'est-ce qu'un pulsar?

1. étoile à neutrons
   objet compact de compacité $\frac{R_s}{R_*} \approx 0.4$
   $\Rightarrow$ effets de champ gravitationnel fort
2. fortement magnétisée
   $\Rightarrow$ plasmas quantiques, effets d'EDQ
   (création de paires $e^{\pm}$, raies cyclotron)
3. en rotation plus ou moins rapide
   $\Rightarrow$ intense champ électrique induit
   $\Rightarrow$ accélération violente de particules

Qu'est-ce qu'un pulsar?

1. étoile à neutrons
   objet compact de compacité $\frac{R_s}{R_*} \approx 0.4$
   $\Rightarrow$ effets de champ gravitationnel fort
2. fortement magnétisée
   $\Rightarrow$ plasmas quantiques, effets d'EDQ
   (création de paires $e^{\pm}$, raies cyclotron)
3. en rotation plus ou moins rapide
   $\Rightarrow$ intense champ électrique induit
   $\Rightarrow$ accélération violente de particules

Qu'est-ce qu'un pulsar?

1. étoile à neutrons
   objet compact de compacité $\frac{R_s}{R_*} \approx 0.4$
   $\Rightarrow$ effets de champ gravitationnel fort
2. fortement magnétisée
   $\Rightarrow$ plasmas quantiques, effets d'EDQ
   (création de paires $e^\pm$, raies cyclotron)
3. en rotation plus ou moins rapide
   $\Rightarrow$ intense champ électrique induit
   $\Rightarrow$ accélération violente de particules

Magnétosphère des pulsars: généralités

Qu'est-ce qu'un pulsar?

1. étoile à neutrons
   objet compact de compacité $\frac{R_s}{R_*} \approx 0.4$
   $\Rightarrow$ effets de champ gravitationnel fort
2. fortement magnétisée
   $\Rightarrow$ plasmas quantiques, effets d'EDQ
   (création de paires $e^{\pm}$, raies cyclotron)
3. en rotation plus ou moins rapide
   $\Rightarrow$ intense champ électrique induit
   $\Rightarrow$ accélération violente de particules

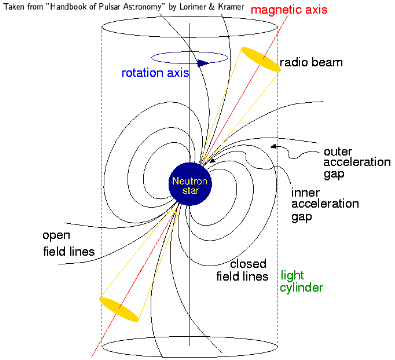

(Lorimer & Kramer, Handbook of pulsar astronomy)

Magnétosphère des pulsars: généralités

Qu'est-ce qu'un pulsar?

1. étoile à neutrons
   objet compact de compacité $\frac{R_S}{R_*} \approx 0.4$
   $\Rightarrow$ effets de champ gravitationnel fort
2. fortement magnétisée
   $\Rightarrow$ plasmas quantiques, effets d'EDQ (création de paires $e^{\pm}$, raies cyclotron)
3. en rotation plus ou moins rapide
   $\Rightarrow$ intense champ électrique induit
   $\Rightarrow$ accélération violente de particules

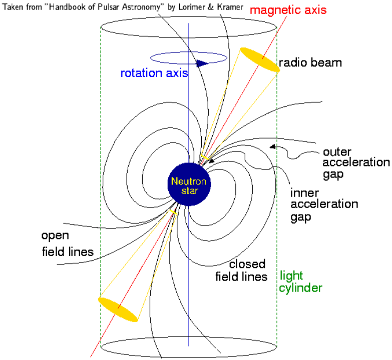

(Lorimer & Kramer, Handbook of pulsar astronomy)

Quelques définitions utiles

- obliquité χ: angle entre moment magnétique $\vec{\mu}_*$ et axe de rotation $\vec{\Omega}_*$
- rotateur aligné / perpendiculaire / oblique: $\chi = 0$ / 90^o / quelconque
- rayon du cylindre lumière: surface sur laquelle une particule en corotation avec l'étoile atteint la vitesse de la lumière $r_L = c/\Omega_*$
  $\Rightarrow$ transition entre un régime quasi-statique et la zone d'onde

Les grandes classes de pulsars

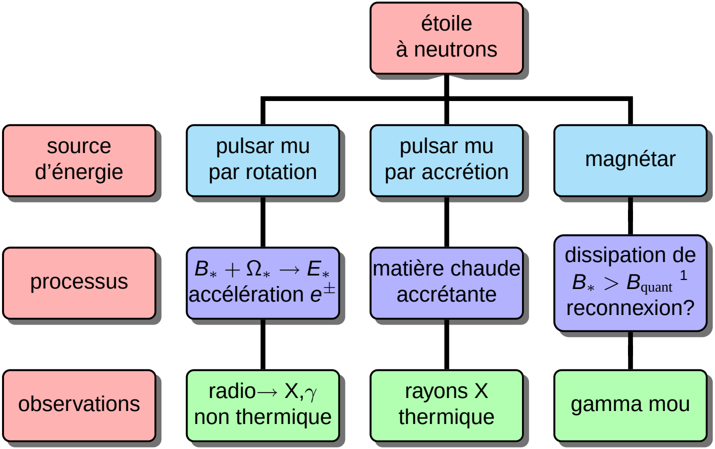

$\Rightarrow$ distinction par la source d'énergie à l'origine de l'activité de l'étoile à neutrons

[1] champ magnétique quantique $B_{\rm quant} = 4.4 \times 10^9$ T pour lequel $\hbar\,\omega_{B_{\rm quant}} = m_e c^2$

Magnétosphère des pulsars: ordres de grandeur

Des observations

- période de rotation $P \in [1.5\ ms, 10\ s]$
- dérivée de la période $\dot{P} \in [10^{-18}, 10^{-15}]$
- perte par freinage rotationnel contraint par

$$L_{\rm sd} = 4\,\pi^2\,I_*\,\dot{P}\,P^{-3} \approx 10^{24} - 10^{31}\ W$$

  très différent des trous noirs ou des étoiles à neutrons accrétantes (taux d'accrétion $\dot{M}$ inconnu)
- champ magnétique estimé par rayonnement dipolaire magnétique

$$B_*\ \sin\chi = 3.2\times10^{15}\ \mathrm{T}\ \sqrt{P\,\dot{P}} = 10^5 - 10^8\ \mathrm{T}$$

  $\Rightarrow$ ne contraint que $B_\perp$
  $\Rightarrow$ valeur cohérente avec la conservation du flux magnétique lors de l'effondrement du progéniteur

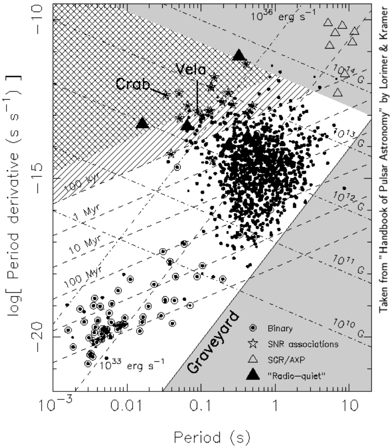

(Lorimer & Kramer)

Magnétosphère des pulsars: ordres de grandeur

- champ électrique induit au niveau de la croûte stellaire

$$E_* = \Omega_* B_* R_* = 10^{13}\ \mathrm{V/m}$$

$\Rightarrow$ accélération “instantanée” à des vitesses ultra-relativistes, facteur de Lorentz $\gamma \gg 1$ ($\tau_{\mathrm{acc}} < 10^{-20}$ s)

- force d'attraction gravitationnelle négligeable !!

$$\frac{F_{\mathrm{grav}}}{F_{\mathrm{em}}} \approx \frac{G\,M_*\,m_p/R_*^2}{e\,\Omega_*\,B_*\,R_*} \approx 10^{-12} \ll 1 \tag{1}$$

$\Rightarrow$ dynamique de la magnétosphère dominée par le champ électromagnétique

Sur les caractéristiques de l'étoile à neutrons

- masse de $M_* \approx 1.4\,M_\odot$
- rayon de $R_* \approx 10$ km
- densité centrale de $\rho_c \approx 10^{17}\ \mathrm{kg/m^3}$

Pulsars gammas: l'apport de Fermi/LAT

- plus d'une centaine de pulsars gamma connus à ce jour (en constante augmentation)
  (a) jeunes et énergétiques visibles dans tout le spectre (Crabe)
  (b) jeunes et n'émettant pas/n'étant pas visible? en radio (Geminga)
  (c) millisecondes
- courbes de lumière en forme de double pic pour 75% d'entre eux, séparation des pics de 0.2 en phase
- flux au-delà de 100 MeV approxilativement $dN/dE \approx 10^{-8}\ \mathrm{ph/cm^2/s}$
- spectre moyen (intégré sur la période) en loi de puissance + coupure exponentielle

$$\frac{dN}{dE} \propto E^{-\Gamma} e^{-E/E_{\mathrm{cut}}} \quad (2)$$

$\Gamma \approx 1 - 2$ tandis que la coupure $E_{\mathrm{cut}} \approx 1 - 5$ GeV. Cet ajustement me semble douteux.

- luminosité rotationnelle $L_{\mathrm{sd}} \approx 10^{26} - 10^{31}$ W
- luminosité gamma L_γ entre 0.1% et 100% de L_{sd}
  => $L_\gamma \lesssim L_{\mathrm{sd}}$, on atteint les limites de la conservation de l'énergie!
- la coupure spectral informe sur les mécanisme et sites de production du rayonnement, pense-t-on!?

(Abdo et al, ApJS, 2009)

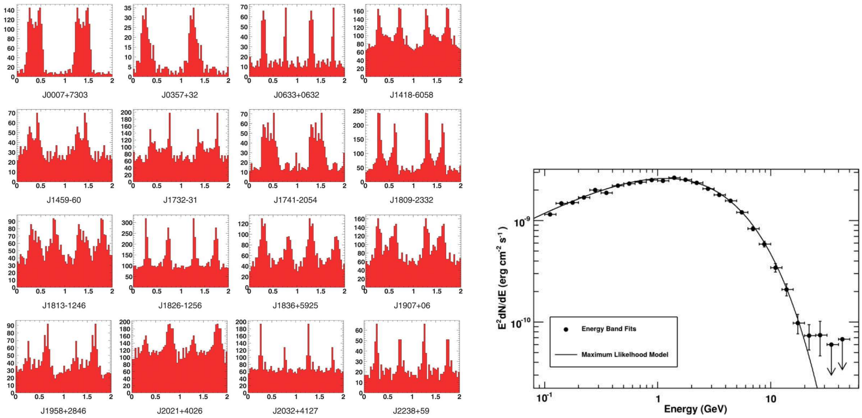

Figure: Courbe de lumière de quelques pulsars gammas, à gauche, (Abdo et al, Science 2009) et spectre moyen de Vela, à droite (Abdo et al, 2010).

Catalogue des pulsars gamma: positionnement

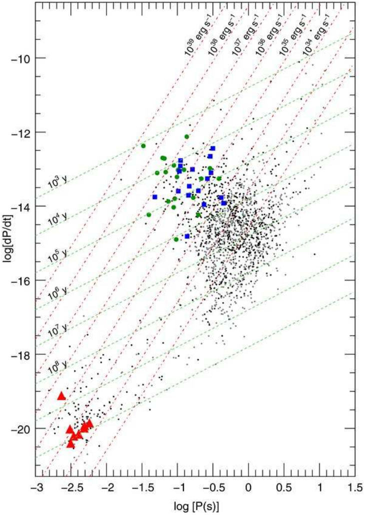

Figure: Le diagramme $P - \dot{P}$ des pulsars Fermi issus du 1er catalogue (Abdo et al. 2010)

Catalogue des pulsars gamma: luminosité

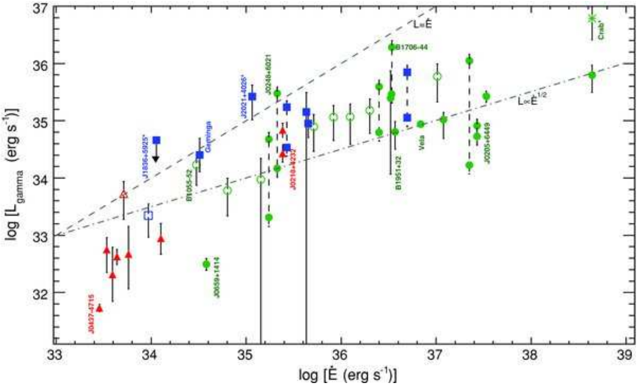

Figure: La luminosité gamma des pulsars Fermi issus du 1er catalogue (Abdo et al, 2010).

- détection de l'émission pulsée du Crabe à 50-400 GeV par MAGIC/VERITAS
- compatible avec le spectre dans la bande Fermi
- spectre en double loi de puissance plutôt que coupure exponentielle

=> spectre brisé avec fréquence de cassure et non de coupure

=> remet en cause les modèles d'émission magnétosphérique

=> presque tous les modèles actuels défunts !

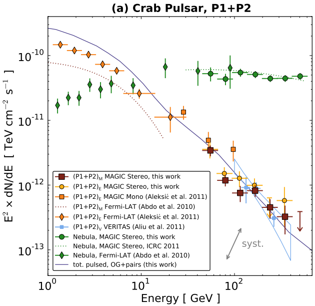

Figure: Émission pulsée du Crabe (Aleksic et al. 2012).

UNIVERSITÉ DE STRASBOURG

Magnétosphère force-free

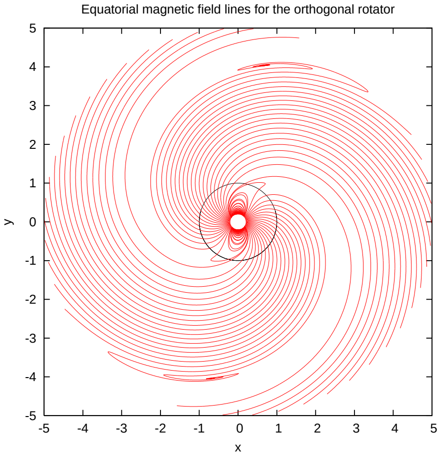

Figure: Lignes de champ magnétique.

Rotateur perpendiculaire (Pétri, MNRAS 2012a)

Magnétosphère force-free

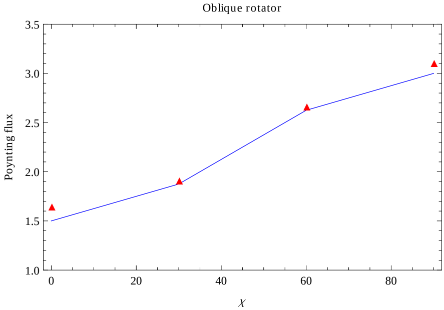

Figure: Luminosité rotationnelle

Perte d'énergie rotationnelle $L_{\rm sd}$ (Pétri, MNRAS 2012a)

$$L_{\rm sd} \approx \frac{3}{2} L_{\rm dip}^{\perp} (1 + \sin^2 \chi) \quad (3)$$

Formule plus réaliste que celle du dipole magnétique dans le vide ($B_\perp$ ET $B_\parallel$ contraints)

The split monopole solution

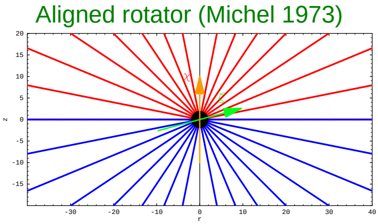

- Definition
  - two half monopoles
  - equal and opposite magnetic moment
  - each located in one half-space (depicted in red and blue).
- Properties
  - exact analytical solution exists
  - asymptotic structure as an archimedean spiral, $B_\varphi \propto 1/r$
  - magnetic polarity change in the equatorial plane
    $\Rightarrow$ formation of a current sheet $\equiv$ stripe

The striped wind structure

Asymptotic MHD solution: oblique rotator (Bogovalov 1999)

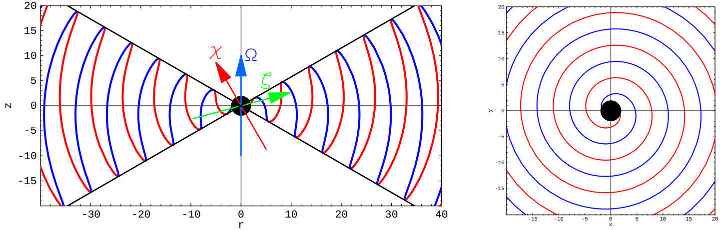

- Definition
  - Ω: rotation axis
  - χ: inclination of magnetic axis
  - ζ: inclination of line of sight.
- Properties
  - assumes only $B_\varphi \propto 1/r$
  - independent of the magnetospheric structure inside the light cylinder
  - discontinuous magnetic polarity reversal
    $\Rightarrow$ infinitely thin current sheet $\equiv$ striped wind
    (more realistic model = finite thickness)

1. What? Objectives
   - high-energy pulsed emission (>10 MeV)
   - spectral variability of several gamma-ray pulsars.
2. How?
   - synchrotron radiation from hot and magnetized plasma in the stripe
   - IC with target photons
     - cosmic microwave background, CMB
     - synchrotron photons from the nebula, X-ray
     - thermal emission from the neutron star surface, black body with $T_{\rm bb} \approx 10^6$ K
     - photons from companion star
3. To whom? Applications
   - isolated pulsars
     gamma ray pulsars
   - binary pulsars
     application to PSR B1259-63
4. link to other wavelengths? radio band?
   - polar cap for radio emission: phenomenological
   - striped wind for gamma rays (Mev-GeV)

$\Rightarrow$ geometry well defined.

High-energy emission from gamma-ray pulsars

2. How?
   - synchrotron radiation from hot and magnetized plasma in the stripe

3. To whom? Applications
   - isolated pulsars
     gamma ray pulsars

2. How?
   - photons from companion star
3. To whom? Applications
   - binary pulsars
     application to PSR B1259-63

UNIVERSITÉ DE STRASBOURG

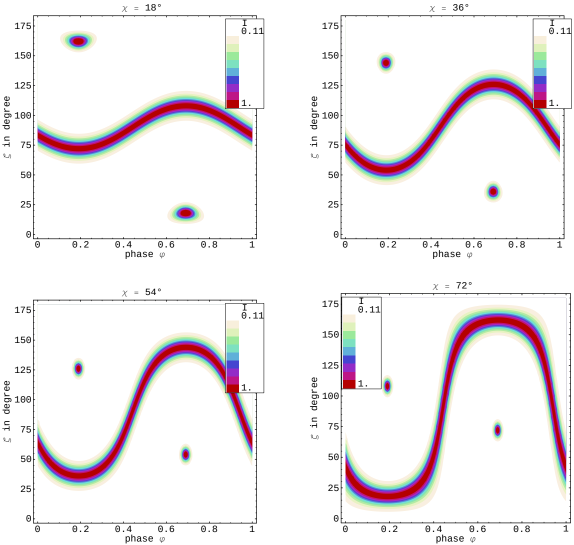

(Pétri, MNRAS, 2011)

Radio time lag and gamma-ray peak separation

From pure geometric considerations

Gamma-ray peak separation Δ

$$\cos(\pi\,\Delta) = |\cot\zeta\;\cot\chi|$$

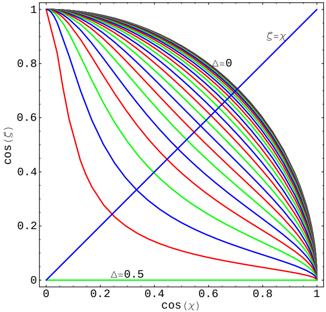

Radio time lag δ

$$\delta \approx \frac{1-\Delta}{2}$$

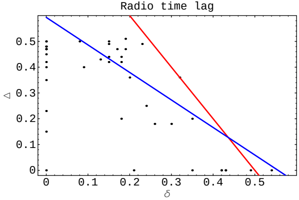

(Pétri, MNRAS, 2011)

Main results

- S-shape reflects emission from current sheets
- two spots corresponding to polar cap emission (north & south pole separated by half a period)
- several light-curve combinations possible depending on geometry χ, ζ
  - no pulse !
  - only radio
  - only gamma
  - one radio + one/two gamma-ray pulse(s)
  - two radio pulse
    => perpendicular rotator, $\zeta \approx \chi \approx 90^o$

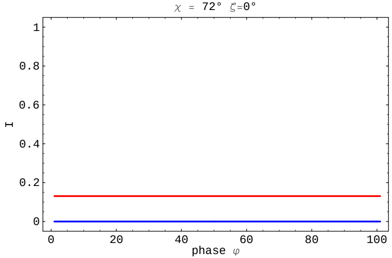

(Pétri, MNRAS, 2011)

Main results

- S-shape reflects emission from current sheets
- two spots corresponding to polar cap emission (north & south pole separated by half a period)
- several light-curve combinations possible depending on geometry χ, ζ
  - no pulse !
  - only radio
  - only gamma
  - one radio + one/two gamma-ray pulse(s)
  - two radio pulse
    => perpendicular rotator, $\zeta \approx \chi \approx 90^o$

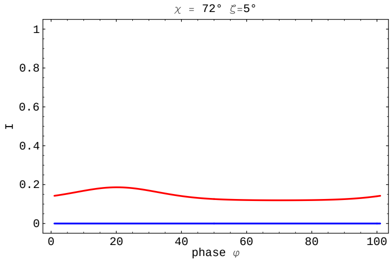

(Pétri, MNRAS, 2011)

Relation between radio and gamma-ray pulses

Main results

- S-shape reflects emission from current sheets
- two spots corresponding to polar cap emission (north & south pole separated by half a period)
- several light-curve combinations possible depending on geometry χ, ζ
  - no pulse !
  - only radio
  - only gamma
  - one radio + one/two gamma-ray pulse(s)
  - two radio pulse
    => perpendicular rotator, $\zeta \approx \chi \approx 90^o$

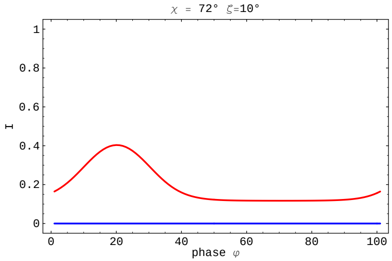

(Pétri, MNRAS, 2011)

Relation between radio and gamma-ray pulses

Main results

- S-shape reflects emission from current sheets
- two spots corresponding to polar cap emission (north & south pole separated by half a period)
- several light-curve combinations possible depending on geometry χ, ζ
  - no pulse !
  - only radio
  - only gamma
  - one radio + one/two gamma-ray pulse(s)
  - two radio pulse
    => perpendicular rotator, $\zeta \approx \chi \approx 90^o$

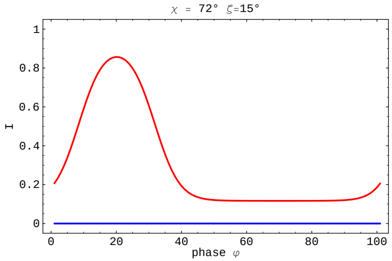

(Pétri, MNRAS, 2011)

Main results

- S-shape reflects emission from current sheets
- two spots corresponding to polar cap emission (north & south pole separated by half a period)
- several light-curve combinations possible depending on geometry χ, ζ
  - no pulse !
  - only radio
  - only gamma
  - one radio + one/two gamma-ray pulse(s)
  - two radio pulse
    => perpendicular rotator, $\zeta \approx \chi \approx 90^o$

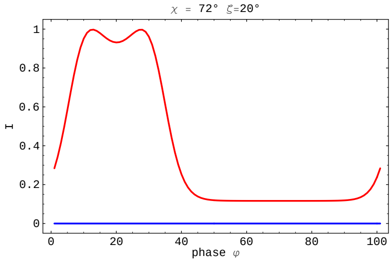

(Pétri, MNRAS, 2011)

Relation between radio and gamma-ray pulses

Main results

- S-shape reflects emission from current sheets
- two spots corresponding to polar cap emission (north & south pole separated by half a period)
- several light-curve combinations possible depending on geometry χ, ζ
  - no pulse !
  - only radio
  - only gamma
  - one radio + one/two gamma-ray pulse(s)
  - two radio pulse
    => perpendicular rotator, $\zeta \approx \chi \approx 90^o$

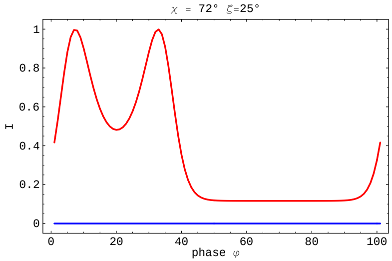

(Pétri, MNRAS, 2011)

Relation between radio and gamma-ray pulses

Main results

- S-shape reflects emission from current sheets
- two spots corresponding to polar cap emission (north & south pole separated by half a period)
- several light-curve combinations possible depending on geometry χ, ζ
  - no pulse !
  - only radio
  - only gamma
  - one radio + one/two gamma-ray pulse(s)
  - two radio pulse
    => perpendicular rotator, $\zeta \approx \chi \approx 90^o$

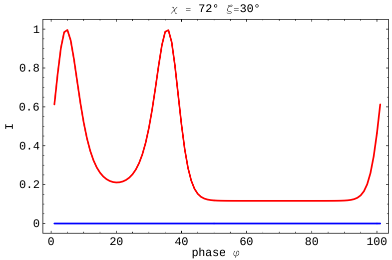

(Pétri, MNRAS, 2011)

Relation between radio and gamma-ray pulses

Main results

- S-shape reflects emission from current sheets
- two spots corresponding to polar cap emission (north & south pole separated by half a period)
- several light-curve combinations possible depending on geometry χ, ζ
  - no pulse !
  - only radio
  - only gamma
  - one radio + one/two gamma-ray pulse(s)
  - two radio pulse
    => perpendicular rotator, $\zeta \approx \chi \approx 90^o$

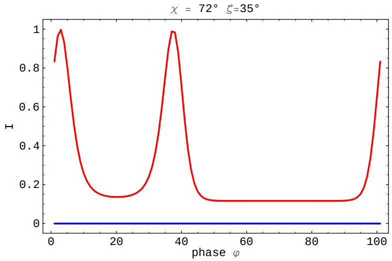

(Pétri, MNRAS, 2011)

Main results

- S-shape reflects emission from current sheets
- two spots corresponding to polar cap emission (north & south pole separated by half a period)
- several light-curve combinations possible depending on geometry χ, ζ
  - no pulse !
  - only radio
  - only gamma
  - one radio + one/two gamma-ray pulse(s)
  - two radio pulse
    => perpendicular rotator, $\zeta \approx \chi \approx 90^o$

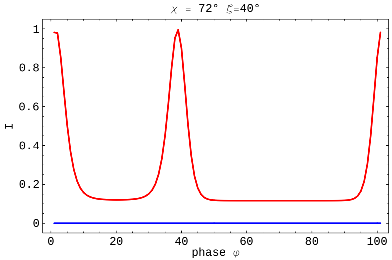

(Pétri, MNRAS, 2011)

Relation between radio and gamma-ray pulses

Main results

- S-shape reflects emission from current sheets
- two spots corresponding to polar cap emission (north & south pole separated by half a period)
- several light-curve combinations possible depending on geometry χ, ζ
  - no pulse !
  - only radio
  - only gamma
  - one radio + one/two gamma-ray pulse(s)
  - two radio pulse
    => perpendicular rotator, $\zeta \approx \chi \approx 90^o$

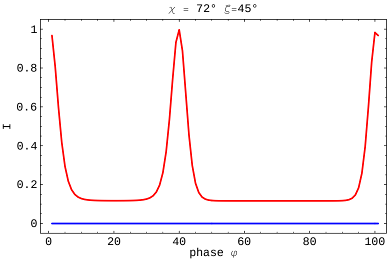

(Pétri, MNRAS, 2011)

Relation between radio and gamma-ray pulses

Main results

- S-shape reflects emission from current sheets
- two spots corresponding to polar cap emission (north & south pole separated by half a period)
- several light-curve combinations possible depending on geometry χ, ζ
  - no pulse !
  - only radio
  - only gamma
  - one radio + one/two gamma-ray pulse(s)
  - two radio pulse
    => perpendicular rotator, $\zeta \approx \chi \approx 90^o$

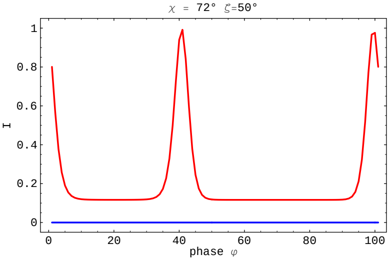

(Pétri, MNRAS, 2011)

Relation between radio and gamma-ray pulses

Main results

- S-shape reflects emission from current sheets
- two spots corresponding to polar cap emission (north & south pole separated by half a period)
- several light-curve combinations possible depending on geometry χ, ζ
  - no pulse !
  - only radio
  - only gamma
  - one radio + one/two gamma-ray pulse(s)
  - two radio pulse
    => perpendicular rotator, $\zeta \approx \chi \approx 90^o$

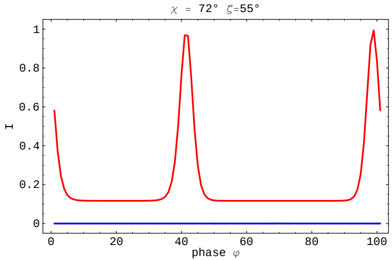

(Pétri, MNRAS, 2011)

Relation between radio and gamma-ray pulses

Main results

- S-shape reflects emission from current sheets
- two spots corresponding to polar cap emission (north & south pole separated by half a period)
- several light-curve combinations possible depending on geometry χ, ζ
  - no pulse !
  - only radio
  - only gamma
  - one radio + one/two gamma-ray pulse(s)
  - two radio pulse
    => perpendicular rotator, $\zeta \approx \chi \approx 90^o$

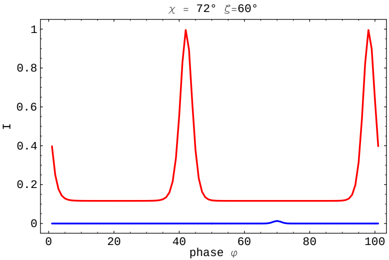

(Pétri, MNRAS, 2011)

Main results

- S-shape reflects emission from current sheets
- two spots corresponding to polar cap emission (north & south pole separated by half a period)
- several light-curve combinations possible depending on geometry χ, ζ
  - no pulse !
  - only radio
  - only gamma
  - one radio + one/two gamma-ray pulse(s)
  - two radio pulse
    => perpendicular rotator, $\zeta \approx \chi \approx 90^o$

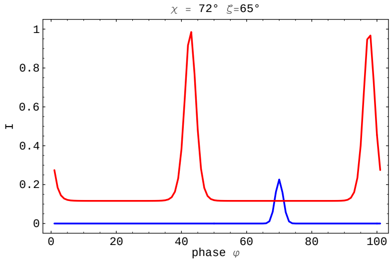

(Pétri, MNRAS, 2011)

Relation between radio and gamma-ray pulses

Main results

- S-shape reflects emission from current sheets
- two spots corresponding to polar cap emission (north & south pole separated by half a period)
- several light-curve combinations possible depending on geometry χ, ζ
  - no pulse !
  - only radio
  - only gamma
  - one radio + one/two gamma-ray pulse(s)
  - two radio pulse
    => perpendicular rotator, $\zeta \approx \chi \approx 90^o$

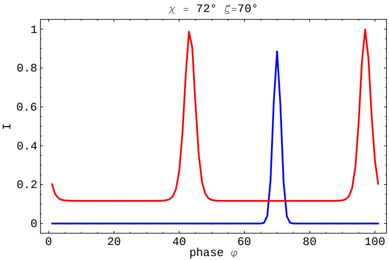

(Pétri, MNRAS, 2011)

Relation between radio and gamma-ray pulses

Main results

- S-shape reflects emission from current sheets
- two spots corresponding to polar cap emission (north & south pole separated by half a period)
- several light-curve combinations possible depending on geometry χ, ζ
  - no pulse !
  - only radio
  - only gamma
  - one radio + one/two gamma-ray pulse(s)
  - two radio pulse
    => perpendicular rotator, $\zeta \approx \chi \approx 90^o$

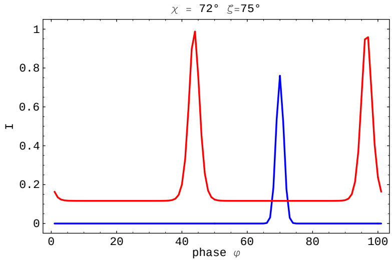

(Pétri, MNRAS, 2011)

Relation between radio and gamma-ray pulses

Main results

- S-shape reflects emission from current sheets
- two spots corresponding to polar cap emission (north & south pole separated by half a period)
- several light-curve combinations possible depending on geometry χ, ζ
  - no pulse !
  - only radio
  - only gamma
  - one radio + one/two gamma-ray pulse(s)
  - two radio pulse
    => perpendicular rotator, $\zeta \approx \chi \approx 90^o$

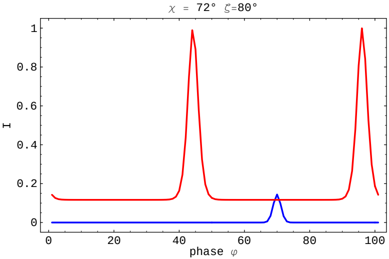

(Pétri, MNRAS, 2011)

Relation between radio and gamma-ray pulses

Main results

- S-shape reflects emission from current sheets
- two spots corresponding to polar cap emission (north & south pole separated by half a period)
- several light-curve combinations possible depending on geometry χ, ζ
  - no pulse !
  - only radio
  - only gamma
  - one radio + one/two gamma-ray pulse(s)
  - two radio pulse
    => perpendicular rotator, $\zeta \approx \chi \approx 90^o$

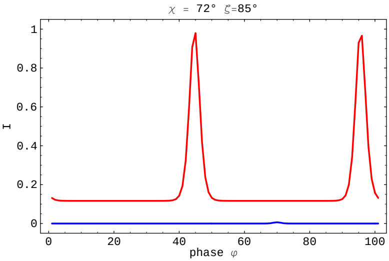

(Pétri, MNRAS, 2011)

Relation between radio and gamma-ray pulses

Main results

- S-shape reflects emission from current sheets
- two spots corresponding to polar cap emission (north & south pole separated by half a period)
- several light-curve combinations possible depending on geometry χ, ζ
  - no pulse !
  - only radio
  - only gamma
  - one radio + one/two gamma-ray pulse(s)
  - two radio pulse
    => perpendicular rotator, $\zeta \approx \chi \approx 90^o$

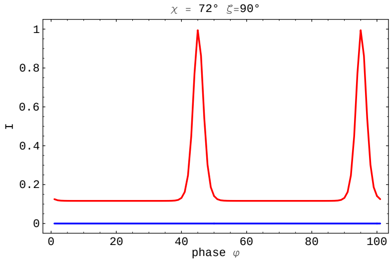

(Pétri, MNRAS, 2011)

Relation between radio and gamma-ray pulses

Main results

- S-shape reflects emission from current sheets
- two spots corresponding to polar cap emission (north & south pole separated by half a period)
- several light-curve combinations possible depending on geometry χ, ζ
  - no pulse !
  - only radio
  - only gamma
  - one radio + one/two gamma-ray pulse(s)
  - two radio pulse
    => perpendicular rotator, $\zeta \approx \chi \approx 90^o$

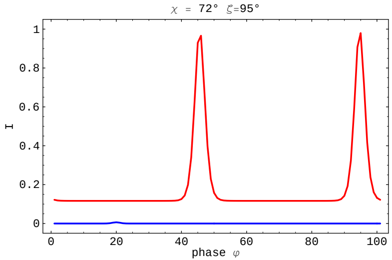

(Pétri, MNRAS, 2011)

Relation between radio and gamma-ray pulses

Main results

- S-shape reflects emission from current sheets
- two spots corresponding to polar cap emission (north & south pole separated by half a period)
- several light-curve combinations possible depending on geometry χ, ζ
  - no pulse !
  - only radio
  - only gamma
  - one radio + one/two gamma-ray pulse(s)
  - two radio pulse
    => perpendicular rotator, $\zeta \approx \chi \approx 90^o$

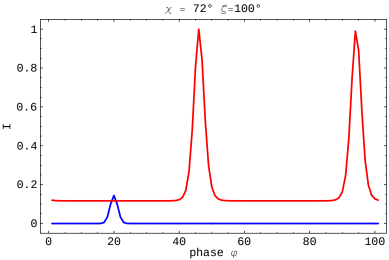

(Pétri, MNRAS, 2011)

Relation between radio and gamma-ray pulses

Main results

- S-shape reflects emission from current sheets
- two spots corresponding to polar cap emission (north & south pole separated by half a period)
- several light-curve combinations possible depending on geometry χ, ζ
  - no pulse !
  - only radio
  - only gamma
  - one radio + one/two gamma-ray pulse(s)
  - two radio pulse
    => perpendicular rotator, $\zeta \approx \chi \approx 90^o$

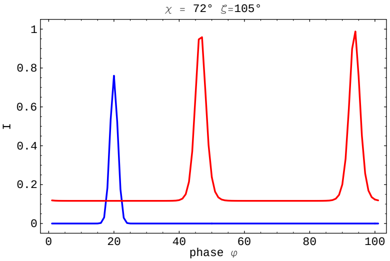

(Pétri, MNRAS, 2011)

Relation between radio and gamma-ray pulses

Main results

- S-shape reflects emission from current sheets
- two spots corresponding to polar cap emission (north & south pole separated by half a period)
- several light-curve combinations possible depending on geometry χ, ζ
  - no pulse !
  - only radio
  - only gamma
  - one radio + one/two gamma-ray pulse(s)
  - two radio pulse
    => perpendicular rotator, $\zeta \approx \chi \approx 90^o$

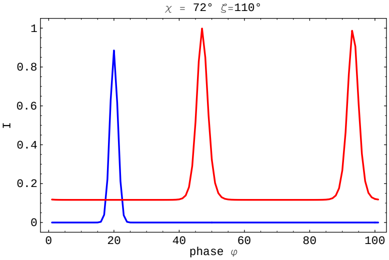

(Pétri, MNRAS, 2011)

Relation between radio and gamma-ray pulses

Main results

- S-shape reflects emission from current sheets
- two spots corresponding to polar cap emission (north & south pole separated by half a period)
- several light-curve combinations possible depending on geometry χ, ζ
  - no pulse !
  - only radio
  - only gamma
  - one radio + one/two gamma-ray pulse(s)
  - two radio pulse
    => perpendicular rotator, $\zeta \approx \chi \approx 90^o$

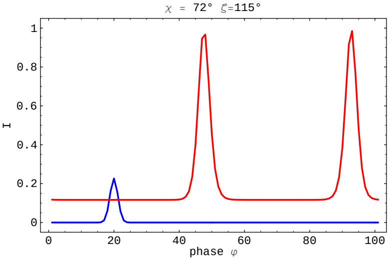

(Pétri, MNRAS, 2011)

Relation between radio and gamma-ray pulses

Main results

- S-shape reflects emission from current sheets
- two spots corresponding to polar cap emission (north & south pole separated by half a period)
- several light-curve combinations possible depending on geometry χ, ζ
  - no pulse !
  - only radio
  - only gamma
  - one radio + one/two gamma-ray pulse(s)
  - two radio pulse
    => perpendicular rotator, $\zeta \approx \chi \approx 90^o$

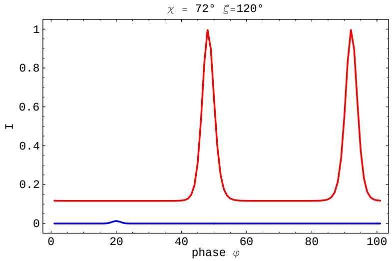

(Pétri, MNRAS, 2011)

Relation between radio and gamma-ray pulses

Main results

- S-shape reflects emission from current sheets
- two spots corresponding to polar cap emission (north & south pole separated by half a period)
- several light-curve combinations possible depending on geometry χ, ζ
  - no pulse !
  - only radio
  - only gamma
  - one radio + one/two gamma-ray pulse(s)
  - two radio pulse
    => perpendicular rotator, $\zeta \approx \chi \approx 90^o$

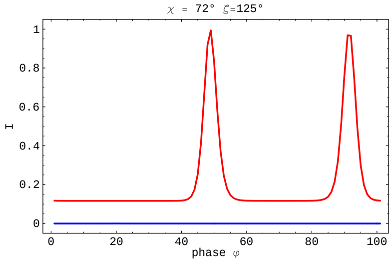

(Pétri, MNRAS, 2011)

Relation between radio and gamma-ray pulses

Main results

- S-shape reflects emission from current sheets
- two spots corresponding to polar cap emission (north & south pole separated by half a period)
- several light-curve combinations possible depending on geometry χ, ζ
  - no pulse !
  - only radio
  - only gamma
  - one radio + one/two gamma-ray pulse(s)
  - two radio pulse
    => perpendicular rotator, $\zeta \approx \chi \approx 90^o$

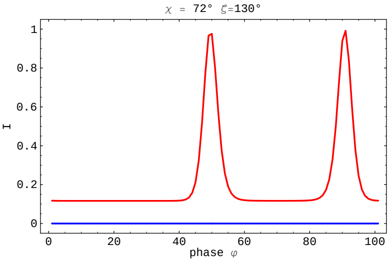

(Pétri, MNRAS, 2011)

Relation between radio and gamma-ray pulses

Main results

- S-shape reflects emission from current sheets
- two spots corresponding to polar cap emission (north & south pole separated by half a period)
- several light-curve combinations possible depending on geometry χ, ζ
  - no pulse !
  - only radio
  - only gamma
  - one radio + one/two gamma-ray pulse(s)
  - two radio pulse
    => perpendicular rotator, $\zeta \approx \chi \approx 90^o$

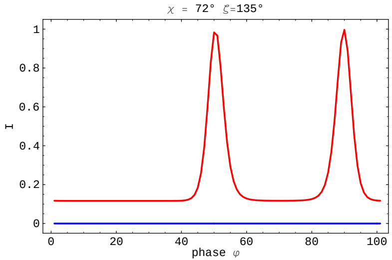

(Pétri, MNRAS, 2011)

Relation between radio and gamma-ray pulses

Main results

- S-shape reflects emission from current sheets
- two spots corresponding to polar cap emission (north & south pole separated by half a period)
- several light-curve combinations possible depending on geometry χ, ζ
  - no pulse !
  - only radio
  - only gamma
  - one radio + one/two gamma-ray pulse(s)
  - two radio pulse
    => perpendicular rotator, $\zeta \approx \chi \approx 90^o$

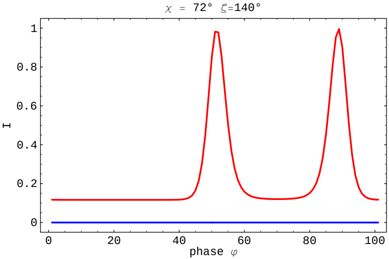

(Pétri, MNRAS, 2011)

Relation between radio and gamma-ray pulses

Main results

- S-shape reflects emission from current sheets
- two spots corresponding to polar cap emission (north & south pole separated by half a period)
- several light-curve combinations possible depending on geometry χ, ζ
  - no pulse !
  - only radio
  - only gamma
  - one radio + one/two gamma-ray pulse(s)
  - two radio pulse
    => perpendicular rotator, $\zeta \approx \chi \approx 90^o$

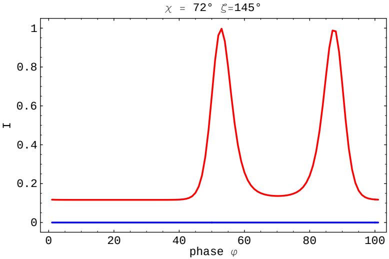

(Pétri, MNRAS, 2011)

Relation between radio and gamma-ray pulses

Main results

- S-shape reflects emission from current sheets
- two spots corresponding to polar cap emission (north & south pole separated by half a period)
- several light-curve combinations possible depending on geometry χ, ζ
  - no pulse !
  - only radio
  - only gamma
  - one radio + one/two gamma-ray pulse(s)
  - two radio pulse
    => perpendicular rotator, $\zeta \approx \chi \approx 90^o$

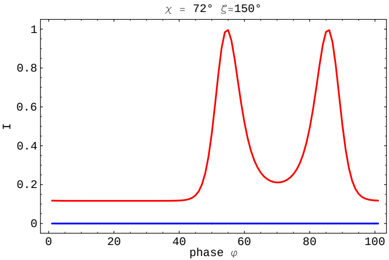

(Pétri, MNRAS, 2011)

Relation between radio and gamma-ray pulses

Main results

- S-shape reflects emission from current sheets
- two spots corresponding to polar cap emission (north & south pole separated by half a period)
- several light-curve combinations possible depending on geometry χ, ζ
  - no pulse !
  - only radio
  - only gamma
  - one radio + one/two gamma-ray pulse(s)
  - two radio pulse
    => perpendicular rotator, $\zeta \approx \chi \approx 90^o$

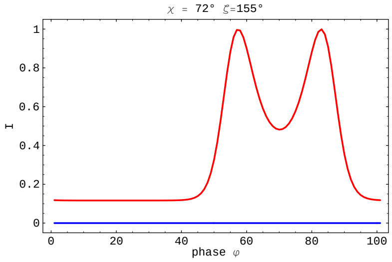

(Pétri, MNRAS, 2011)

Relation between radio and gamma-ray pulses

Main results

- S-shape reflects emission from current sheets
- two spots corresponding to polar cap emission (north & south pole separated by half a period)
- several light-curve combinations possible depending on geometry χ, ζ
  - no pulse !
  - only radio
  - only gamma
  - one radio + one/two gamma-ray pulse(s)
  - two radio pulse
    => perpendicular rotator, $\zeta \approx \chi \approx 90^o$

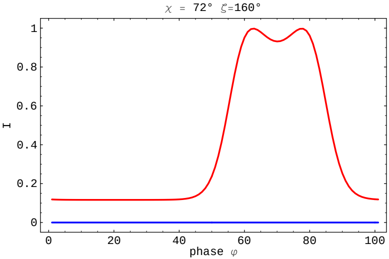

(Pétri, MNRAS, 2011)

Main results

- S-shape reflects emission from current sheets
- two spots corresponding to polar cap emission (north & south pole separated by half a period)
- several light-curve combinations possible depending on geometry χ, ζ
  - no pulse !
  - only radio
  - only gamma
  - one radio + one/two gamma-ray pulse(s)
  - two radio pulse
    => perpendicular rotator, $\zeta \approx \chi \approx 90^o$

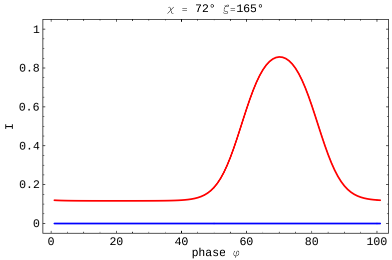

(Pétri, MNRAS, 2011)

Relation between radio and gamma-ray pulses

Main results

- S-shape reflects emission from current sheets
- two spots corresponding to polar cap emission (north & south pole separated by half a period)
- several light-curve combinations possible depending on geometry χ, ζ
  - no pulse !
  - only radio
  - only gamma
  - one radio + one/two gamma-ray pulse(s)
  - two radio pulse
    => perpendicular rotator, $\zeta \approx \chi \approx 90^o$

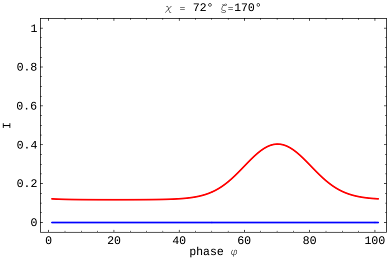

(Pétri, MNRAS, 2011)

Relation between radio and gamma-ray pulses

Main results

- S-shape reflects emission from current sheets
- two spots corresponding to polar cap emission (north & south pole separated by half a period)
- several light-curve combinations possible depending on geometry χ, ζ
  - no pulse !
  - only radio
  - only gamma
  - one radio + one/two gamma-ray pulse(s)
  - two radio pulse
    => perpendicular rotator, $\zeta \approx \chi \approx 90^o$

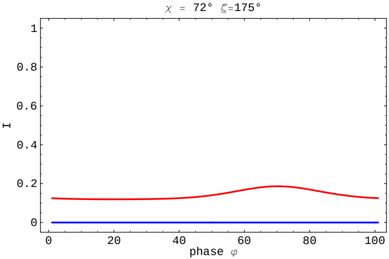

(Pétri, MNRAS, 2011)

Main results

- S-shape reflects emission from current sheets
- two spots corresponding to polar cap emission (north & south pole separated by half a period)
- several light-curve combinations possible depending on geometry χ, ζ
  - no pulse !
  - only radio
  - only gamma
  - one radio + one/two gamma-ray pulse(s)
  - two radio pulse
    => perpendicular rotator, $\zeta \approx \chi \approx 90^o$

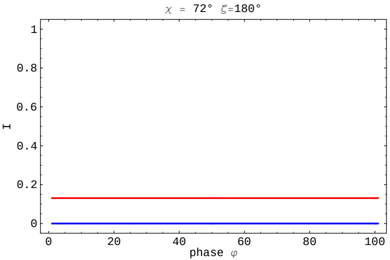

(Pétri, MNRAS, 2011)

Qu'en est-il de la luminosité?

Hypothèses

- émission synchrotron dans la partie striée
  - partie froide et fortement magnétisée peu rayonnante
  - partie chaude et faiblement magnétisée très rayonnante
- refroidissement radiatif compensé par réaccélération par reconnexion magnétique

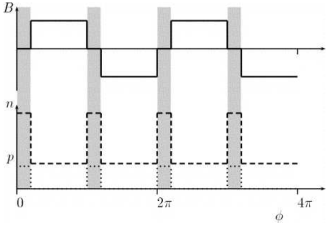

Lyubarsky & Kirk, 2001

Le modèle: l'écoulement de plasma

- équilibre hydrodynamique dans les stries (pression magnétique = pression cinétique)

$$\frac{1}{3}\,\gamma_{\rm h}'\,n_{\rm h}'\,m_{\rm e}\,c^2 = \frac{B'^2}{2\,\mu_0} \quad (4)$$

- énergie rotationnelle injectée dans l'accélération des particules => écoulement d'un plasma froid avec facteur de Lorentz $\Gamma_{\rm v}$ et une efficacité de conversion η

$$\Gamma_{\rm v}\,n_{\rm c}\,m_{\rm e}\,c^2 = \eta\,\frac{L_{\rm sd}}{4\,\pi\,r^2\,c} \quad (5)$$

- injection des particules au niveau des calottes polaires avec un facteur de multiplicité κ

$$\dot{N}_{\pm} \approx 2.77\times10^{30}\ {\rm s}^{-1}\,\kappa\,\left(\frac{P}{1\ s}\right)^{-2}\left(\frac{B_{\rm ns}}{10^8\ {\rm T}}\right)\left(\frac{R_{\rm ns}}{10\ {\rm km}}\right)^3 \quad (6)$$

- lien entre $\Gamma_{\rm v}$ κ et $L_{\rm sd}$

$$\Gamma_{\rm v}\,\kappa \approx 8.7\times10^{8}\,\eta\,\left(\frac{L_{\rm sd}}{10^{28}\ {\rm W}}\right)^{1/2} \quad (7)$$

efficacité et magnétisation

$$(1+\sin^2\chi)\,\sigma\,\eta = 1 \quad (8)$$

- facteur de Lorentz des particules dans le vent (pertes radiatives = dissipation magnétique)

$$\gamma'_{\rm h} = \sqrt{\frac{3}{2}\,\frac{\mu_0\,e\,c}{\sigma_T\,B'_L}\,\frac{r}{r_{\rm L}}\,\tau_{\rm rec}} \qquad (9)$$

- énergie des photons dans le référentiel du vent

$$\varepsilon'_B = \frac{3}{2}\,\gamma'^2_{\rm h}\,\frac{B'}{B_q}\,m_{\rm e}\,c^2 = \frac{9}{4}\,\frac{\mu_0\,e\,m_{\rm e}\,c^3}{\sigma_T\,B_q}\,\tau_{\rm rec} \qquad (10)$$

- énergie des photons dans le référentiel du labo

$$\varepsilon_B = 2\,\Gamma_{\rm v}\,\varepsilon'_B = 472\ \mathrm{MeV}\,\Gamma_{\rm v}\,\tau_{\rm rec}\,. \qquad (11)$$

- facteur de Lorentz du vent

$$\Gamma_{\rm v} \approx 10\, \tau_{\rm rec}^{1/5} \left(\frac{L_{\rm sd}}{10^{28}\ \rm W} \right)^{1/2}$$

- luminosité gamma

$$L_\gamma \approx 2\times 10^{26}\ {\rm W} \left(\frac{L_{\rm sd}}{10^{28}\ \rm W} \right)^{1/2} \left(\frac{P}{1\ \rm s} \right)^{-1/2}$$

(Pétri, MNRAS, 2012b)

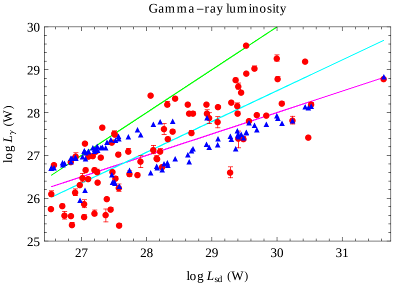

Principaux résultats: taux de reconnexion

$$\tau_{\rm rec} \approx \left(\frac{4.72 \text{ GeV}}{E_{\rm cut}(\text{GeV})} \right)^{-5/6} \left(\frac{L_{\rm sd}}{10^{28} \text{ W}} \right)^{-5/12}$$

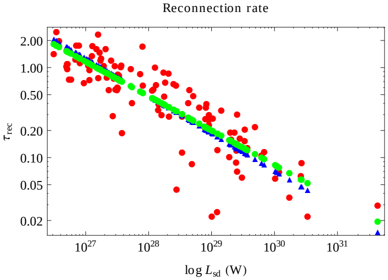

UNIVERSITÉ DE STRASBOURG

Principaux résultats: ligne d'extinction

Condition pour observer une émission pulsée

$$\frac{L_{\rm sd}}{P} \geq 10^{27}\ \mathrm{W/s}$$

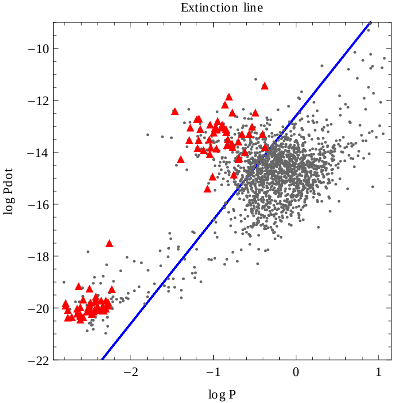

1. Vous avez dit pulsar?
   - remarques générales
   - émission haute énergie
2. La magnétosphère
3. The striped wind
4. Results
   - emission pattern and geometry
   - Luminosité gamma
5. **Magnetic reconnection**
   - The wind problem
   - Plasma instabilities
   - The termination shock
6. Conclusion & perspectives

The wind problem

Description of the system

- in the vicinity of the pulsar, an intense magnetic field, kinetic energy of the particles weak
  $\Rightarrow$ dynamics dominated by the electromagnetic field
- in the nebula, a weak magnetic field, and ultra-relativistic particles responsible for the synchrotron radiation
  $\Rightarrow$ dynamics dominated by the particles

An essential parameter: the magnetisation "σ"

$$\sigma = \frac{\text{Poynting flux}}{\text{particle enthalpy flux}} \approx \frac{\text{electromagnetic energy density}}{\text{particle (kinetic + rest mass) energy density}}$$

A fundamental problem

How to convert the electromagnetic energy into kinetic energy for the particles ?
How to do the transition between the neutron star, $\sigma \gg 1$, to the nebula, $\sigma \ll 1$?

Idea

Magnetic energy dissipation at the termination shock of a striped wind.

Magnetic reconnection

Goal

Study the mechanism of magnetic reconnection in the pulsar wind:

- acceleration of the wind;
- magnetic energy conversion into kinetic energy for the particles.

Method

- analytical and semi-analytical
  - linear study of the electromagnetic instabilities by solving numerically the linearised Vlasov-Maxwell equations;
  - find the condition for magnetic field dissipation when the wind crosses the termination shock
- numerical: PIC simulations.

Applications

- instabilities in relativistic plasmas
- relativistic Harris current sheet
- striped wind
- gamma-ray bursts

Kinetic structure of the striped wind

Composition of the wind

- $e^{\pm}$ pairs in drift motion equal but opposite in direction
- relativistic speeds.

Description of the structure of a stripe

Exact solution: the relativistic Harris current sheet

- magnetic field:
  $B_z(x) = B_0 \tanh(x/a)$;
- particle density of each species:
  $n(x) = N_s \operatorname{sech}^2(x/a)$;
- temperature:
  $\Theta = k_B T_s / m c^2$;
- distribution function of the particles:
  $$f(x, \vec{p}) = \frac{n(x)}{4 \pi m^3 c^3 \Theta K_2(1/\Theta)} e^{-\Gamma_s (E \pm c \beta_s p_y)/\Theta m c^2} .$$

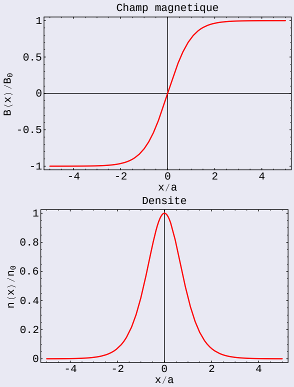

Magnetic reconnection: kinetic approach

Vlasov-Maxwell equation

$$\frac{\partial f}{\partial t} + \vec{v} \cdot \frac{\partial f}{\partial \vec{r}} + q\,(\vec{E} + \vec{v} \wedge \vec{B}) \cdot \frac{\partial f}{\partial \vec{p}} = 0$$

The perturbation of f_s is computed by numerical integration of the trajectories of the particles along the equilibrium orbits. Charge and current densities are obtained by integration over the momentum (by Gauss-Hermite quadrature).

Eigenvalue system

For the electromagnetic potential $(\phi, \vec{A})$

$$\begin{aligned} \phi''(x) - \left(k^2 - \frac{\omega^2}{c^2}\right) \phi(x) + \frac{\rho(x)}{\varepsilon_0} &= 0 \\ \vec{A}''(x) - \left(k^2 - \frac{\omega^2}{c^2}\right) \vec{A}(x) + \mu_0 \vec{j}(x) &= 0 \end{aligned}$$

- charge density: $\rho(x) \propto \sum_s \int_{\mathbb{R}^3} f_s(x, \vec{p})\, d^3\vec{p}$
- current density: $\vec{j}(x) \propto \sum_s \int_{\mathbb{R}^3} \vec{v}\, f_s(x, \vec{p})\, d^3\vec{p}$

Magnetic reconnection: kinetic approach (2)

Growth rate of the two-stream and tearing mode instabilities

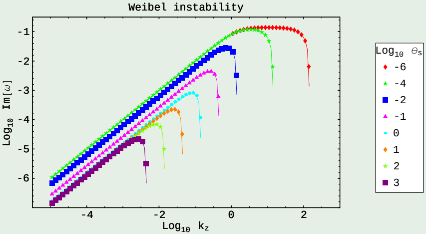

(Pétri & Kirk, 2007a, PPCF)

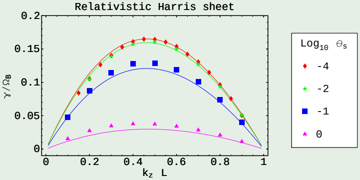

(Pétri & Kirk, 2007b, PPCF)

Magnetic reconnection: kinetic approach (2)

Growth rate of the two-stream and tearing mode instabilities

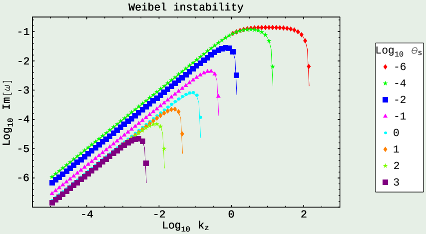

(Pétri & Kirk, 2007a, PPCF)

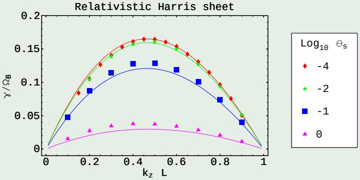

(Pétri & Kirk, 2007b, PPCF)

⇒ this study should help to estimate the reconnection rate in the striped wind.

MHD approach: method

Principle

- striped wind structure preserved
  ⇒ Rankine-Hugoniot relations for the jump in the spatially averaged MHD quantities
  ⇒ conservation of particles, energy and momentum (over one period of the wind)
- the shock region is not described physically.

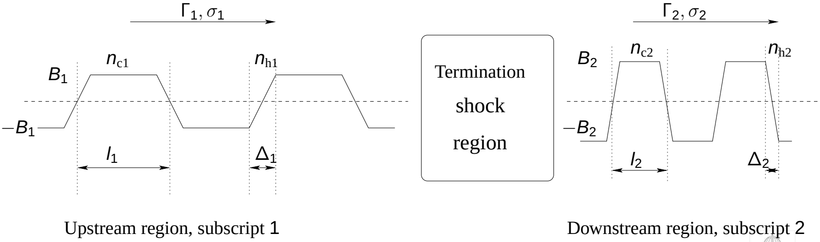

MHD approach: analytical results

Only one free parameter ξ

Relates the downstream current sheet thickness to the downstream Larmor radius (subscript 2)

$$\delta_2 = \xi \, r_{\rm B2}$$

where $\xi > 1$.

Ultra-relativistic limit $(\Gamma_1, \sigma_1) \gg 1$

$$\delta_2 + \frac{1}{4\,\sigma_1} = \frac{1}{4\,\Gamma_2^2}$$

- for $\sigma_1 \gg \frac{5\,l_1}{\xi\,r_{\rm B1}}$, full dissipation: $\delta_2 \approx 1, \Gamma_2 \approx 1$
- for $\sigma_1 \ll \left(\frac{5\,l_1}{4\,\xi\,r_{\rm B1}}\right)^{2/3}$, negligible dissipation: $\delta_2 \ll 1$, $\Gamma_2 \approx \sqrt{\sigma_1} \Rightarrow$ ideal MHD

UNIVERSITÉ DE STRASBOURG

MHD approach: semi-analytical results

Numerical resolution

Numerical search for the MHD jump condition in the most general case for which the upstream magnetisation σ_1 is arbitrary.
Search for the roots of a system of non-linear equations
$\Rightarrow$ needs a good first guess for the solution (therefore the previous analytical study)

The magnetisation σ_2/σ_1

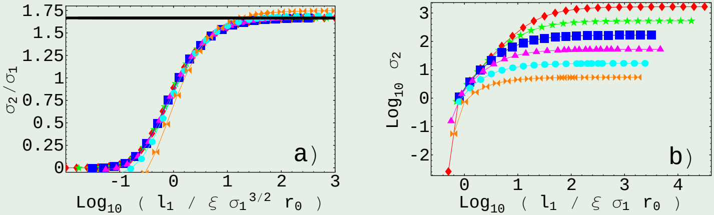

- $\sigma_2/\sigma_1 \ll 1$, almost full dissipation
- $\sigma_2/\sigma_1 \approx 2$, negligible dissipation

PIC simulation: negligible dissipation with $\sigma = 3$, $\Gamma = 20$

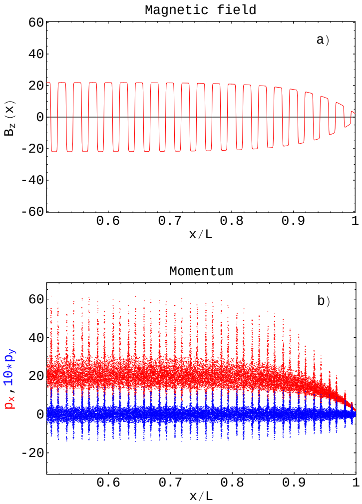

PIC simulations: full dissipation with $\sigma = 45$, $\Gamma = 20$

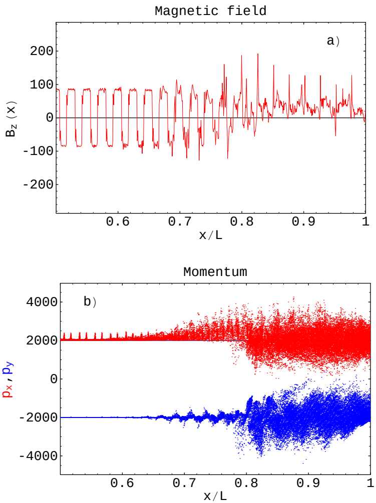

(Pétri & Lyubarsky, A&A, 2007)

Synthesis of the PIC simulations

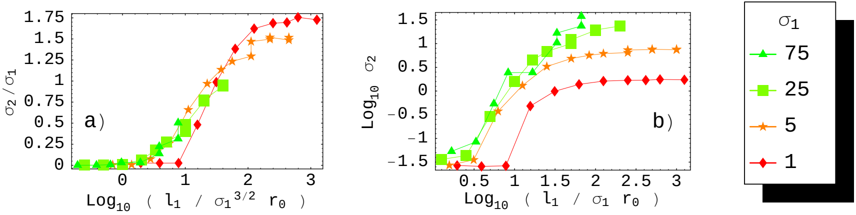

From this we deduce the parameter ξ introduced in the analytical model: $\xi \approx 10$

Magnetic reconnection at the termination shock

significant if the analytical criterion is satisfied

- for $l_1/r_{\mathrm{B1}}\,\sigma_1 \leq 3$, full dissipation, downstream flow purely hydrodynamical, $\Gamma_2 \approx 1$, particles heated to relativistic temperatures
- for $\sigma_1 \leq (l_1/12\,r_{\mathrm{B1}})^{2/3}$, no reconnection. Striped wind structure is preserved, simple compression, $\Gamma_2 = \sqrt{\sigma_1}$

Conclusions & perspectives

Pulsed emission

- high-energy pulsed emission emanating from regions outside the light cylinder, $r \approx (1 - 100)\, r_{\mathrm{L}}$
- gamma-ray luminosities from Fermi/LAT second source explained by synchrotron emission/reconnection in the stripe

Further investigations

- link between asymptotic toroidal magnetic field and magnetosphere $\Rightarrow$ location where most of the high-energy pulsed emission is expected
- refinement of the model to include recent Fermi detections
- phase-resolved polarisation properties in X-ray
- possible explanation for gamma-ray binaries
- population study

Isolated vs binary pulsars

What changes?

- location of the termination shock
- strong external target photon field from companion
- variation with orbital phase

The case of PSR B1259-63

Pulsar parameters

- period $P = 47.7$ ms
- $L_{\rm sd} = 8.3 \times 10^{28}$ W

Feature of the companion Be star known

- $L_* = 3.3 \times 10^{30}$ W
- $\dot{M} = 10^{-8} \, M_\odot/yr$
- $v_{\rm wind} = 1000$ km/s
- separation $d = 9.6 \times 10^{10}$ m to 1.2×10^{12} m

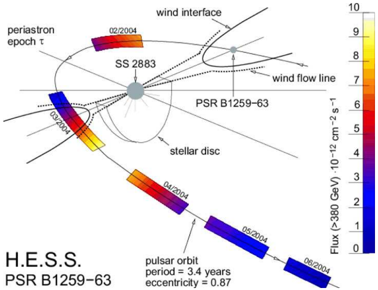

Aharonian et al (2005)

Termination shock

pressure balance implies

$$\frac{R_{\rm TS}}{R_{\rm w}} = \sqrt{\frac{L_{\rm sd}}{\dot{M} \, v_{\rm w} \, c}} \approx 0.7$$

PSR B1259-63: what can we learn?

Orbital phase variability

- phase-averaged light-curve depends on orbital phase
- maximum at periastron
- spectral variability with orbital phase
  - spectral slope, transition Thomson/Klein-Nishina regime
  - cut-off and break energy

=> special features for pulsars in binaries

Light curve above 100 MeV

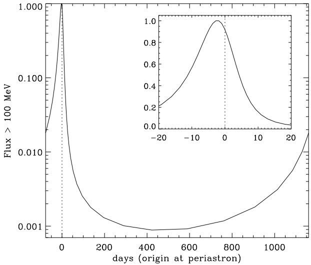

Phase-averaged spectra

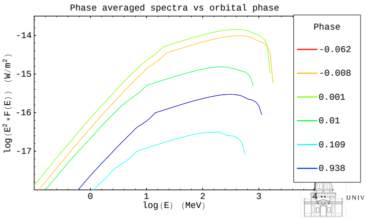

(Pétri & Dubus, MNRAS, 2011)